

## Chapter 24

# BIFURCATIONS

### Abstract

### Keywords:

Phase Portrait  
Fixed Point  
Saddle-Node  
Bifurcation Diagram  
Codimension-1  
Hysteresis  
Hopf Bifurcation  
SNIC

## 24.1 Introduction

In linear systems, responses are proportional to its input: e.g. when a system's input is doubled, so is its output. Obviously this property is overboard when nonlinear dynamics is involved. The nonlinearity may lead to disproportional, and sometimes even counterintuitive changes in the behavior of a system. Another very important property is the existence of sudden qualitative changes in the dynamical behavior due to a parameter change of a nonlinear system. These sudden changes are known as bifurcations. A well-known example of such a bifurcation in neuroscience is the sudden transition of the state of a neuron from the subthreshold state to firing action potentials. In this Chapter we introduce the basics of bifurcations. For an excellent and in depth overview of this topic and application of bifurcation theory to neuronal systems, see Strogatz (1994) and Izhikevich (2007) respectively.

## 24.2 Effects of Parameter Selection on Linear and Nonlinear Systems

For one dimensional dynamics, the mechanism underlying a bifurcation can be envisioned in a combined plot of phase space and the associated dynamics. For example, for the linear case  $\dot{S} = A - S$  and the nonlinear case  $\dot{S} = A - S^2$ , we can plot  $\dot{S}$  as a function of  $S$  and obtain the so-called phase portrait (Fig. 24.1A-F). The change on the phase line at a given location of  $S$ , can be seen in the phase portrait and can also be visualized by putting an imaginary particle, also called a phase point, on the phase line. For example, a phase point at the location  $S = 50$  in Fig. 24.1A will move to the left until it reaches the fixed point at  $S = 25$ .

In panels A and B in Figure 24.1, we used the parameter  $A = 25$ . Let us now change the value of parameter  $A$  in both the linear and nonlinear case (Fig, 24.1C-F). In the linear case the location of the fixed point changes, but the dynamics remains qualitatively the same: i.e. there is still a stable fixed point on the phase line. This fixed point is stable because small perturbations around the fixed point will drive the phase point back to the fixed point. An example of an unstable fixed point is the left fixed point in Fig. 24.1B; here a small perturbation at the fixed point will drive the phase point away from the fixed point.

In contrast to the example for the linear case, the dynamics for the nonlinear system is totally changed: the two fixed points that were present in Figure 24.1B are reduced to a single fixed point in Fig 24.1D, and vanished in Figure 24.1F! In this example, we changed the system's parameter, and its behavior changes qualitatively. In other words, the system has undergone a **bifurcation** due to a change of its parameter  $A$ . Looking at the examples in Figure 24.1, it is clear why one needs nonlinearity to create such a bifurcation: when the relationship between  $S$  and  $\dot{S}$  is a straight line, there will always be an intersection with the abscissa where  $\dot{S} = 0$ , i.e. a fixed point (Fig. 24.1A, C). One could point out that the exception would be when the line moved to an orientation precisely parallel to the phase line; in that case there would not be an intersection, i.e. a fixed point. This observation is correct but this would indicate that  $\dot{S}$  is a constant and no longer a function of  $S$ . In contrast, if the relationship between  $S$  and  $\dot{S}$  is nonlinear, the value of  $A$  and thus the position of the curve determines if there are intersections between that curve and the abscissa where  $\dot{S} = 0$  (Fig. 24.1B, D).

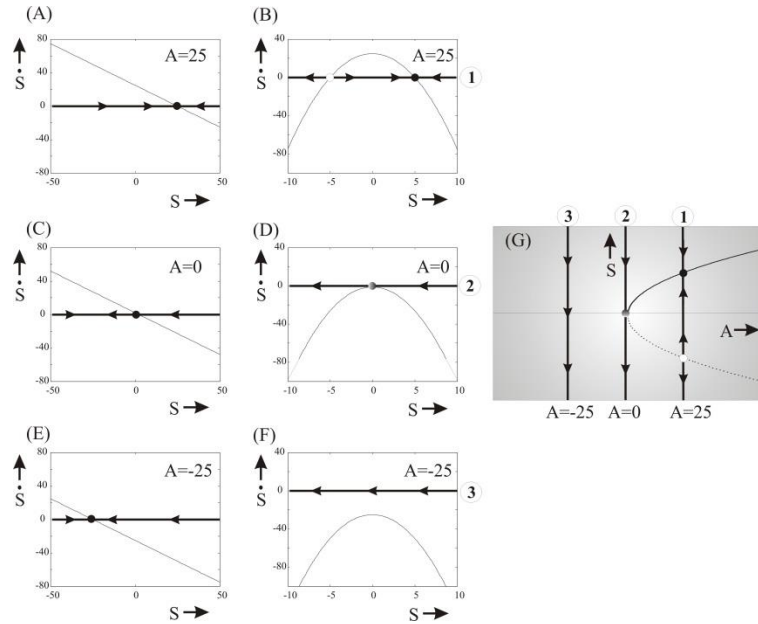


Fig. 24.1

Phase space representation of the parameter dependent dynamics governed by a linear and nonlinear ODE.

(A)  $\dot{S} = A - S$  for  $A = 25$  and (B)  $\dot{S} = A - S^2$  for  $A = 25$ .

(C) and (D) are the same ODEs, but for  $A = 0$ .

(E) and (F) are the same ODEs, but for  $A = -25$ .

Stable fixed points are indicated by solid dots, unstable ones by a circle, and the half stable one in panel (D) with a half solid/half open dot. It can be seen that a change of  $A$  in the linear case moves the position of the stable fixed point (panels A, C and E). In contrast, a change of  $A$  in the nonlinear case has a more dramatic effect: it determines the number of fixed points (panels B, D and F). The bifurcation diagram for the nonlinear case shown in panels (B), (D) and (F) is depicted in panel (G). This diagram is obtained by combining the dynamics on the phase line as a function of the value of the parameter  $A$ . In this example the phase lines denoted by 1, 2, and 3 are shown. The stable fixed points in the bifurcation diagram are located on the solid line while the unstable ones are on the dotted line. The location at  $A = 0$ , where the dynamics changes, is the so-called bifurcation point.

If we determine the behavior of the nonlinear system for a range of parameter values, we can construct a so-called bifurcation diagram (Fig. 24.1G). In this diagram the parameter  $A$  becomes the independent variable, plotted on the abscissa, while the behavior on the  $S$  line is now the dependent variable, plotted on the ordinate. The stable fixed points on the bifurcation diagram are represented by a solid line, while the unstable ones are connected by a dotted line. The phase lines and arrows showing the dynamics as depicted in the example in Fig. 24.1G are usually omitted in bifurcation diagrams.

### 24.3 Codimension-1 Bifurcations on the Phase Line (1D Dynamics)

Although there is a wide variety of possible scenarios that can generate a bifurcation, the number types of bifurcation one can generate on a phase line by changing a single parameter (called the codimension) is limited. That is if one reduces the bifurcations to their prototypical/canonical form (Fig. 24.2).

The subcritical pitchfork bifurcation is not explicitly shown in Fig. 24.2. Although one only needs a third order nonlinear term to create this bifurcation, there is usually a fifth order term

added to the equation in order to create a stability surrounding the instable pitchfork branches. Such a fifth order term leads to hysteresis.

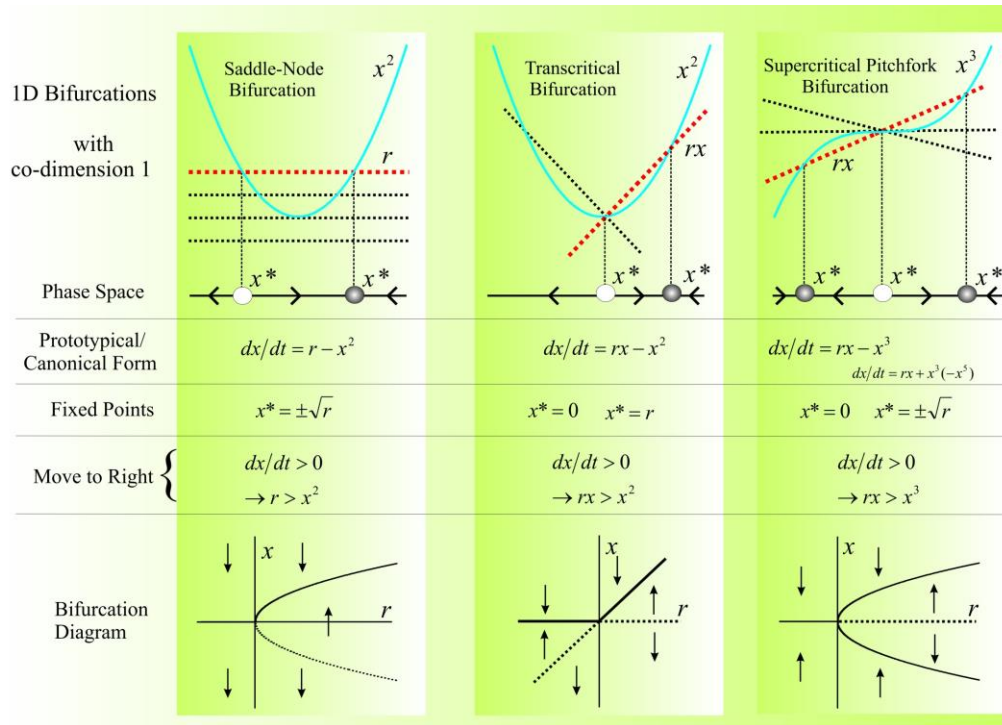


Fig. 24.2

Overview of types of codimension-1 bifurcation on a phase line.

(Left) The saddle-node bifurcation (also called fold-, turning-point-, or blue sky bifurcation)

(Middle) The transcritical bifurcation

(Right) The supercritical pitchfork bifurcation (the equation for the subcritical pitchfork is shown in small font)

## 24.4 Using 1D Dynamics to Model Neural Excitability

Although 1D dynamics is limited for modeling neuronal activity, it is feasible. Two examples are described in the following.

### 24.4.1 Excitability on a Line

The MATLAB routine `pr24_1` uses a simple model with membrane depolarizing and leak currents. This model described in Izhikevich (2007) is a 1D reduction of the Hodgkin and Huxley equations. This results in a membrane characteristic that can undergo a saddle-node bifurcation if sufficient current is injected. Using this script, one can compare the behavior, depending on a number of initial conditions, with `pr24_1(0)` and `pr24_1(60)`; the number in between brackets is the injected current. The shortcoming of this model is that it can only depolarize and if a repolarization is needed for a particular modeling approach, an ad hoc reset of the membrane potential is required. Such an ad hoc reset of the membrane potential is also required in the quadratic integrate-and-fire (QIF) model (CH 30) and the SMC model described by Izhikevich (2007).

### 24.4.2 Excitability on a Circle

If one changes the straight line into a circle, one can still use 1D approach while an oscillation now becomes possible. This approach can be explored with [pr24\\_2](#). In this case the dynamic variable is the phase  $0 \leq \theta < 2\pi$ . This implies that this approach is limited in the sense that it can only be used to model the phase and not the amplitude of an oscillation! In the example in [pr24\\_2](#), the variable  $I$  represents the current input to the neuron.

### 24.5 Using 2D Dynamics to Model Neural Excitability

The formalism for the membrane potential model of the squid's giant axon proposed by Hodgkin and Huxley (1952) (H&H) has shown to be very powerful for simulation of a wide variety of neuronal systems. The original H&H model is **nonlinear** and **4-dimensional** because it contains parameters for membrane potential ( $V$ ), potassium activation ( $n$ ), sodium activation ( $m$ ) and inactivation ( $h$ ). Due to the nonlinearity and high-dimensionality of the model, it must be analyzed with computational methods. To make the neuronal models accessible to mathematical analysis, attempts have been made to simplify the models to fewer dimensions and in some cases to linearize the subthreshold activity (**CH 30**).

A pioneer model in which the neuronal model is reduced to 2-dimensions is the **FitzHugh-Nagumo model** (FitzHugh, 1961; Nagumo et al., 1962). Here the remaining parameters are membrane potential ( $V$ ) and a parameter ( $w$ ) responsible for resetting a depolarized membrane. The latter parameter can be considered to represent potassium activation ( $n$  in H&H), sodium inactivation ( $h$  in H&H) or both. Sodium activation is replaced by its equilibrium value because  $\text{Na}^+$  activation much faster than its inactivation or activation of  $\text{K}^+$ .

Another approach for reduction of the H&H approach is described by Morris and Lecar (1981) and the persistent sodium and potassium model ( **$I_{\text{Na,p}}+I_{\text{K}}$ -model**) described by Izhikevich (2007). Here is an instantaneous depolarizing current ( $\text{Ca}^{++}$  in Morris-Lecar and  $\text{Na}^+$  in Izhikevich) and a slower hyperpolarizing current ( $\text{K}^+$  in both these models). Both models are 2-dimensional: a parameter for membrane potential ( $V$ ) and the  $\text{K}^+$  activation parameter ( $n$ ). In both models there is also a leak current ( $I_L$ ) included. The  $I_{\text{Na,p}}+I_{\text{K}}$ -model can be explored with the MATLAB script [pr24\\_3.m](#).

The common features in the FitzHugh-Nagumo, Morris-Lecar, and  $I_{\text{Na,p}}+I_{\text{K}}$ -models is that they are nonlinear and 2-dimensional. This makes these models accessible for mathematical analysis in the 2D phase plane. Izhikevich (2007) describes the codimension-1 bifurcations that can be observed in these type of 2-dimensional models.

Two examples of the  $I_{\text{Na,p}}+I_{\text{K}}$ -model are shown in Figs. 24.3 and 24.4 which were made by script [pr24\\_3](#). Fig.24.3 is the version with a high-threshold (threshold at  $-25\text{mV}$ ) and slow  $\text{K}^+$  current. It shows the so-called saddle-node on invariant cycle (SNIC) bifurcation between resting and spiking states. The spiking state corresponds with a limit cycle which is drawn **schematically** in Fig. 24.3.

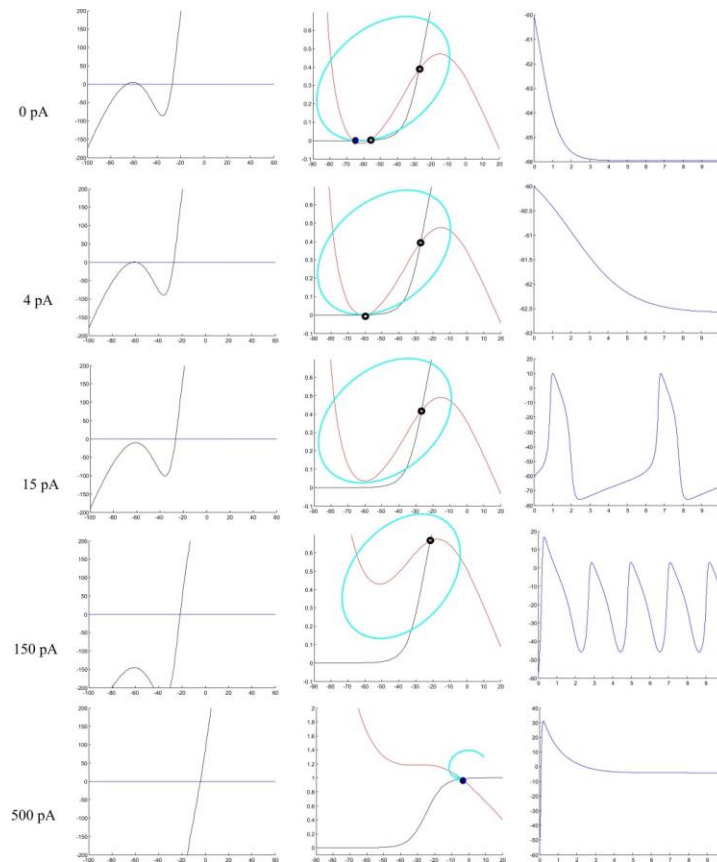


Fig. 24.3

Integrators at different values of current injection: I-V relationship, the null-clines (red – V-null and black – u-null), and the time series computed with the Euler method. From rest to spiking there is a **saddle-node on invariant cycle bifurcation** around  $I=4\text{pA}$  (the spike-amplitude is constant after passing the bifurcation but the frequency of spiking increases with distance from the bifurcation; therefore it is also called the **infinite-period bifurcation** in Strogatz, p. 262); at higher injections the limit cycle changes into saturation (fixed point) via a **supercritical Hopf bifurcation** (the amplitude of the limit cycle decreases toward the bifurcation point and is disappeared at  $I=500\text{ pA}$ . This Figure was created with `pr24_3(InjectionCurrent,-25,-80)`; in which the Injection current was varied between 0 and 500 pA.

NOTE: Limit cycles and trajectories (light blue) are drawn schematically and not based on the precise vector field!

Fig. 24.4 is the version with a low-threshold  $\text{K}^+$  current (threshold at  $-45\text{mV}$ ). It shows the so-called supercritical Hopf bifurcation between resting and spiking states. The spiking state corresponds with a limit cycle which is drawn **schematically** in Fig. 24.4.

Izhikevich shows that depending on the **threshold for  $\text{K}^+$**  ( $V_{1/2}$  for the Boltzman curve) the stable resting potential loses stability on via a saddle-node (high threshold) or a Hopf bifurcation (low threshold). The saddle-node bifurcation can be on an invariant cycle if the **rate of  $\text{K}^+$  activation** ( $\tau_n$ ) is low (shown in Fig. 24.3), or off the cycle if the  $\text{K}^+$  activation is fast (Table 1). The Hopf bifurcation can be supercritical (shown in Fig. 24.4) if the **sodium activation curve** ( $m_\infty$ ) is **not too steep**, or subcritical if the sodium activation is steep (Table 1).

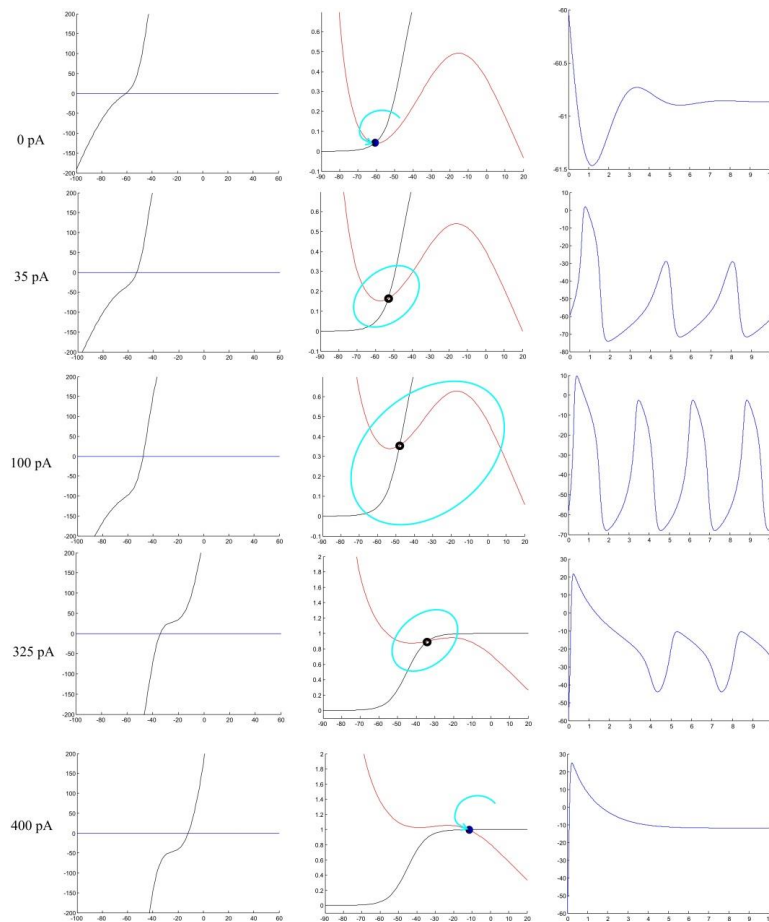


Fig. 24.4

Resonators at different values of current injection: I-V relationship, the null-clines (red – V-null and black – u-null), and the time series computed with the Euler method. From rest to spiking there is **supercritical Hopf bifurcation** (the limit cycle amplitude grows with distance from the bifurcation but the spike frequency only changes slightly with increased current injection); at higher injections the limit cycle changes into saturation (fixed point) via a **supercritical Hopf** (the amplitude of the limit cycle decreases toward the bifurcation point and then disappears. This Figure was created with `pr24_3(InjectionCurrent,-45,-78)`; in which the Injection current was varied between 0 and 400 pA.

NOTE: Limit cycles and trajectories (light blue) are schematically and not based on the precise vector field!

Table 24.1

Overview of the different bifurcations from rest to firing in the  $I_{Na,p}+I_K$ -model.

High Threshold $K^+$ Activation	Slow $K^+$ Activation	Saddle-node on Invariant Cycle (SNIC)
	Fast $K^+$ Activation	Saddle-node
Low Threshold $K^+$ Activation	Steep $Na^+$ Activation	Subcritical Hopf
	No Steep $Na^+$ Activation	Supercritical Hopf

## 24.6 Codimension-2 Bifurcations

The saddle-node, transcritical, pitchfork, Hopf, SNIC bifurcations are all examples of codimension-1 bifurcations, which indicates that we had to vary a single parameter ( $r$  in most cases) to obtain the bifurcation. We can also consider codimension-2 bifurcations in which two parameters must be varied. These sudden transitions were baptized ‘catastrophes’ by René Thom (1972) in his seminal work entitled ‘Stabilité Structurelle et Morphogénèse’; a few years later this work was translated into English (R Thom (1975) – Structural Stability and Morphogenesis, Benjamin/Cummings Publishing Co, Inc., Reading, Massachusetts). In **CH 31** we will consider such an example that can lead to sudden transitions in a network of model neurons using the so-called Ising spin model.

## 24.7 The Epileptor

See:

Jirsa VK, Stacey WC, Quilichini PP, Ivanov AI, Bernard C (2014) - On the nature of seizure dynamics. *Brain* 137: 2210-2230

**Appendix 24.1: Overview of the Codimension-1 Bifurcations in 2D**

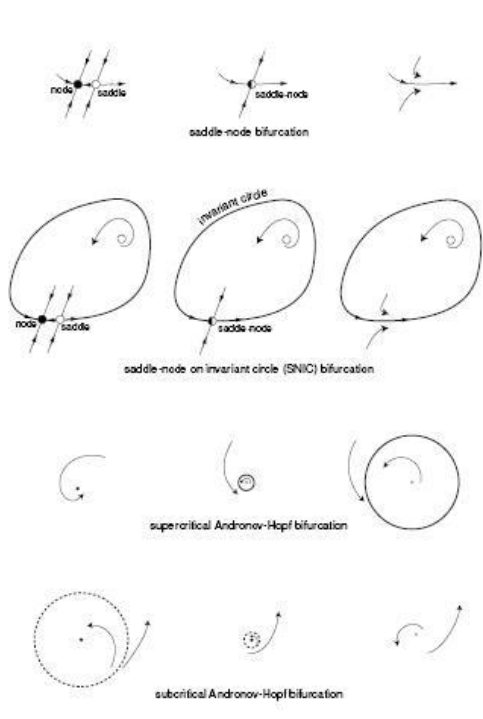


Figure 6.46: Summary of all codimension-1 bifurcations of a stable equilibrium (resting state).

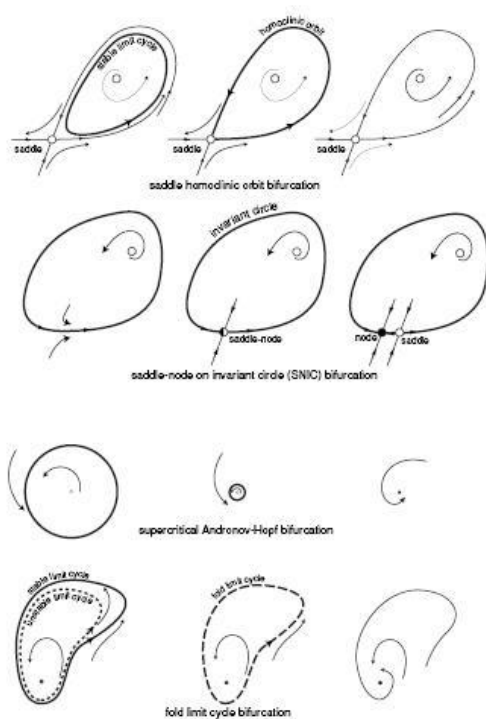


Figure 6.47: Summary of all codimension-1 bifurcations of a stable limit cycle (tonic spiking state) on a plane.

Fig. A24-1

Overview of the codimension-1 bifurcations in neuronal models (After Izhikevich (2007) Figs. 6.46 and 6.47)

Note that in Fig. 6.46, there is no stable limit cycle shown in the subcritical Hopf bifurcation (the stable cycle created by a stabilizing  $r^5$  term), whereas for the inverse (fold) in Fig. 6.47 there is a stable limit cycle surrounding the unstable one shown.